PFG – Journal of Photogrammetry, Remote Sensing and Geoinformation Science
https://doi.org/10.1007/s41064-026-00389-8

RESEARCH

Downscaling Satellite-derived Optical Trapezoid Model with Uncrewed Aerial Vehicle Data for Peatland Water Table Monitoring

Saara Heikkinen[1,2] · Aleksi Räsänen[1] · Anton Kuzmin[3] · Pasi Korpelainen[3] · Timo Kumpula[3] · Aleksi Isoaho[2]

Received: 21 October 2025 / Accepted: 12 March 2026

Abstract
Optical remote sensing, particularly satellite-derived optical trapezoid model (OPTRAM), can be used as a proxy to monitor peatland water table (WT), a key determinant for peatland condition. So far, OPTRAM has been used only in temporal monitoring of WT at coarse spatial resolution while it has not been tested to detect spatial patterns of WT in spatially heterogeneous northern peatlands. To address the abovementioned gap, we downscale four differently parameterized Sentinel-2 OPTRAMs with the help of optical, thermal, and topographic uncrewed aerial vehicle (UAV) variables and random forest modeling in two open peatlands in northern Finland covered by spatially extensive field measurements of WT ($n = 95$). We (1) assess how parameterization of OPTRAM affects OPTRAM-WT correlation, (2) test whether downscaled OPTRAM correlates stronger with WT than the original OPTRAM, and (3) compare OPTRAM to other remote sensing variables calculated from Sentinel-2 and UAV data. Our results showed that OPTRAM parameterization strongly affects OPTRAM-WT correlation, with Spearman correlation (r_s) ranging between 0.23–0.53. Random forest-based downscaling models had a relatively high explained variance (45.6–72.4%). Downscaling increased r_s by 0.09–0.16 units, up to 0.62 with the best-performing parameterization, and revealed the spatial patterns of WT more realistically than Sentinel-2 OPTRAM. Other UAV and Sentinel-2 variables had differing correlations with WT, with greenness and water cover indices having stronger correlations with WT than OPTRAM ($|r_s|$ up to 0.67). Our results encourage the use of downscaling methods at high spatial resolutions and integrating multi-sensor and machine learning methods to generate high spatial and temporal resolution peatland WT monitoring approaches.

Keywords Drones · Remote sensing · Satellite imagery · Soil moisture · Wetland · Uncrewed aerial systems

1 Introduction

Peatlands are undergoing extensive human-induced degradation (Kolari et al. 2022; Leifeld and Menichetti 2018; Sallinen et al. 2019). The degradation has led to negative impacts on greenhouse gas emissions (Alm et al. 2023; Leifeld and Menichetti 2018) and biodiversity (Minkkinen et al. 2008) in peatland ecosystems that in pristine conditions act as globally significant carbon sinks (Yu 2011) and diverse habitats (Steenvoorden and Limpens 2023). Water table (WT) is a commonly used indicator of peatland ecosystem condition as it provides insight into the state of drying and degradation (e.g. Menberu et al. 2016). While there are differences in optimal WT level between peatland types and microforms, in general, low WT indicates a dry and degraded peatland whereas a high WT indicates pristine-like conditions or restoration.

Field-based WT measurements are labor-intensive and challenging in secluded and inaccessible peatlands. In addition, the overarching spatial view of WT variation in peatlands is lacking with point measurements conducted manually or with automated loggers (Haapalehto et al. 2014; Isoaho et al. 2024b). Remote sensing methods, particularly optical sensors, have shown to be an efficient and broad-scale alternative to field-based measurements particularly in open peatlands (Burdun et al. 2023; Isoaho et al. 2023; Jussila et al. 2024; Räsänen et al. 2022). While WT or other phenomena below the ground cannot be measured directly with optical remote sensing data, WT can be assessed in-

✉ Aleksi Räsänen
aleksi.rasanen@oulu.fi

[1] Geography Research Unit, University of Oulu, Oulu, Finland

[2] Natural Resources Institute Finland, Oulu, Finland

[3] Department of Geographical and Historical Studies, University of Eastern Finland, Joensuu, Finland

Published online: 20 March 2026

directly as especially surface moisture and vegetation can and act as proxies for it in peatlands (e.g. Irfan et al. 2020).

Optical sensors can be mounted on different remote sensing platforms. Each have their own advantages and disadvantages, for example, while capturing large geographical areas and producing imagery that is frequently, widely and openly available, satellite imagery is limited by relatively coarse spatial resolution compared to uncrewed aerial vehicle (UAV) data (Atkinson 2013; Campbell et al. 2023; Jussila et al. 2024). UAV data in turn can be collected with a spatial resolution less than a centimeter and a more flexible schedule in contrast to satellite data but is constrained by battery life and weather conditions as well as laborious processing (Lendzioch et al. 2021; Steenvoorden et al. 2023; Steenvoorden and Limpens 2023). Additionally, spectral resolution of common UAV multispectral sensors is lower compared to satellite products. Particularly, UAV cameras often lack shortwave-infrared (SWIR) region that is included in the in the widely used optical satellite datasets, such as Landsat and Sentinel-2, and that has been shown to be important in peatland WT and soil moisture studies (Burdun et al. 2020, 2023; Räsänen et al. 2022, Isoaho et al. 2024b, Reddin et al. 2025).

One method of combining data collected by satellites and UAVs is downscaling, which is defined as increasing of spatial resolution in the field of remote sensing (Atkinson 2013). Through downscaling, smaller pixels and a more detailed spatial image are produced. It is a common method in soil moisture studies, since hydrological changes have often a spatial detail too fine to distinguish with coarse spatial resolution imagery (Abowarda 2021; Fu et al. 2024; Im 2016; Peng et al. 2017).

With downscaling, there is potential to utilize the advantages of both UAV and satellite imagery datasets. It could be possible to model high-resolution spatial variation of SWIR-based variables and produce temporally and spatially high-resolution data by combining UAV imagery depicting high-spatial resolution variation and high temporal resolution satellite imagery with coarser spatial resolution. Furthermore, if satellite-derived observations are reliable and valid, downscaling could even reduce the need for collecting field reference data. Previous studies leveraging downscaling have focused mainly on microwave data with a spatial resolution of kilometers, although downscales of hundreds or tens of meters have also been tested (Abowarda 2021; Babaeian et al. 2019; Im 2016; Jääskeläinen et al. 2025; Li et al. 2021; Mahmood 2024). However, as northern peatlands have fine-scale spatial heterogeneity, monitoring of them requires high spatial resolution, with the necessary pixel size varying between sub-meter to tens of meters depending on the studied phenomena (Isoaho et al. 2024b; Räsänen and Virtanen 2019; Steenvoorden et al. 2023; Steenvoorden and Limpens 2023). Thus, downscaling to a finer spatial resolution requires testing to shed light on its potential in peatland WT monitoring.

One potential WT proxy to be downscaled is the Optical Trapezoid Model (OPTRAM, Sadeghi et al. 2017) that has appeared promising in estimating temporal variations in peatland WT (Burdun et al. 2020, 2023; Räsänen et al. 2022). OPTRAM is shown to be a stabler predictor of WT than spectral indices, with OPTRAM-WT correlations being up to 0.9 (Burdun et al. 2023), suggesting that OPTRAM could function as a universal peatland WT proxy, even with limited amount of field validation data. OPTRAM is parameterized using a trapezoid generated in a scatterplot between the normalized difference vegetation index (NDVI, Tucker 1979) and SWIR transformed reflectance (STR, Sadeghi et al. 2015). The lower and upper edges of the trapezoid represent the so-called dry and wet edges, respectively. The OPTRAM values are a result of a point's vertical distance to the dry edge, divided by the wet edge's distance to the dry edge at the point's NDVI value. Previous studies have shown that OPTRAM parameterization affects its performance in wetness modeling (Sadeghi et al. 2017, 2023; Ambrosone et al. 2020; Mohamadzadeh et al. 2025); therefore, it could be advisable to test different parameter options to delineate wet and dry edges. OPTRAM has so far been utilized mostly in temporal monitoring of peatland WT while it has not been widely tested detecting spatial patterns of WT, yet alone downscaled and compared with WT proxies calculated from optical, thermal, or topographic UAV data (e.g. Ikkala et al. 2022; Isoaho et al. 2023).

To address the abovementioned gap in knowledge, we construct a random forest model to downscale OPTRAM derived from Sentinel-2 satellite imagery with UAV data. Our overall aim is to assess the potential of OPTRAM to depict spatial variation in peatland WT in its downscaled form. Our more specific objectives are: (1) to analyze how parameterization of OPTRAM affects spatial correlation between OPTRAM and peatland WT, (2) to examine whether downscaling with UAV data improves the OPTRAM-WT correlation, and (3) to compare OPTRAM to other Sentinel-2 variables and UAV variables regarding their spatial correlations with peatland WT.

2 Methods

2.1 Study Site and Field Data

We studied two open mires, Välisuo and Matorovansuo, in northern Finland (Fig. 1). Both mires are affected by adjacent drainage. The study sites receive water both from precipitation and as runoff from surrounding slopes, rendering them minerotrophic. Studied peatlands are mostly treeless or sparsely treed with flark-string pattern charac-

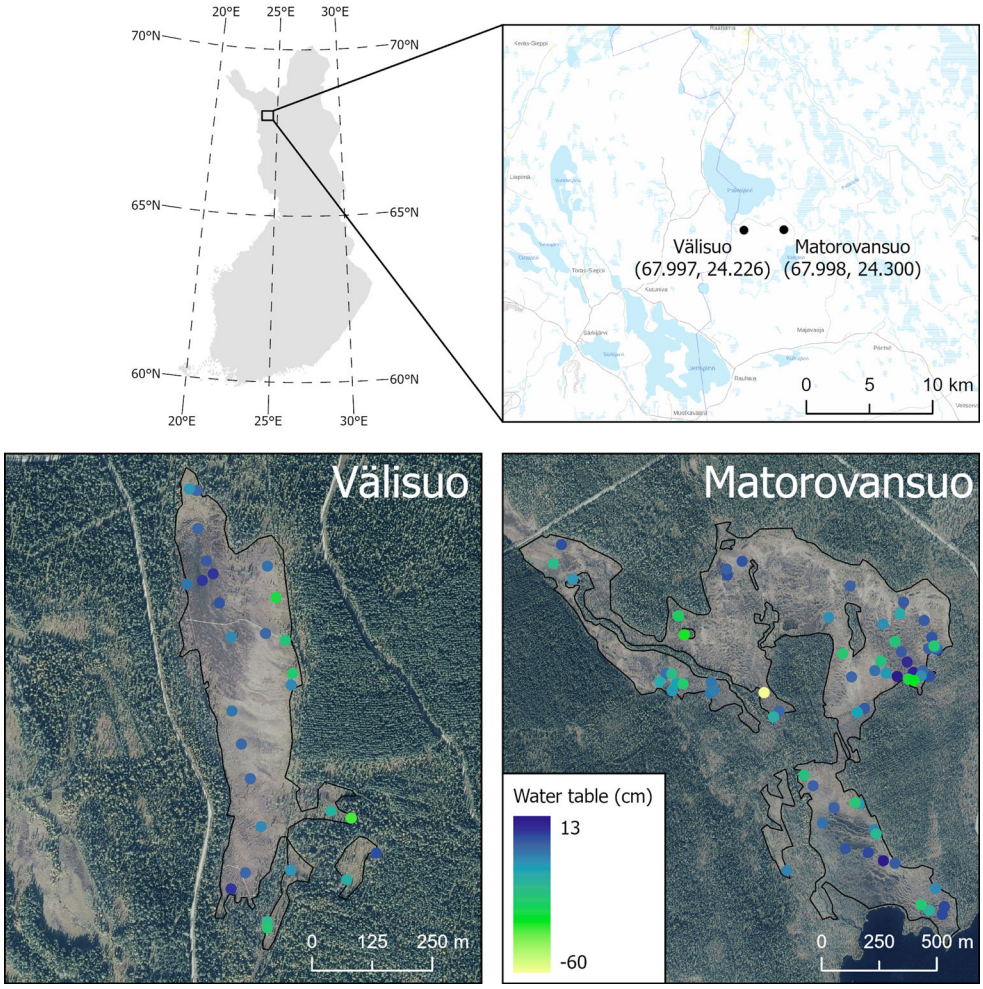

Fig. 1 The locations of the study sites in northern Finland, open mire area delineations and water table measurement points, with measured water table indicated. Background map and aerial images are open data from National Land Survey of Finland

teristic for aapa mires. The wet flarks consist mainly of bare peat and shallow water surfaces with little to no vegetation, although different species of *Carex, Sphagnum*, and wet brown mosses occur. Vegetation on the dry, hummocky strings includes species accustomed to drier conditions such as shrubs and *Sphagnum* and feather mosses; additionally, trees grow in the drier parts of the peatlands. The studied area covers open areas in Välisuo and Matorovansuo, spanning approximately 20 and 110 hectares, respectively.

We collected manual WT measurements during July 23–25, 2023, following the measurement method used earlier (e.g. Haapalehto et al. 2014; Isoaho et al. 2023; Lendzioch et al. 2021). We first inserted a perforated pipe into the peat layer and waited for a couple of days, allowing water to rise to the same level inside the tube as in the surrounding area. We then measured WT relative to the land surface with a centimeter-level accuracy with positive values indicating a WT above and negative below the land surface. We allocated the locations of the WT measurement points using stratified random sampling in which the study sites were first manually divided into sections based mainly on the peatland type. We then randomized three measurement points to each section.

Originally, we measured WT once from 206 points across the sites. As the WT failed to rise to the same level as in the surrounding area in part of the plots located mainly in the drained areas, we utilized only points located in the open areas. Additionally, we did not use measurements taken close to the duckboards, as the duckboards could have interfered the satellite imagery signal. In total we used 95 one-time WT measurements, 28 of which were measured in Välisuo and 67 in Matorovansuo (Fig. 1).

2.2 Remote Sensing Data and Its Preprocessing

We used remote sensing data consisting of satellite and UAV imagery. We acquired the UAV imagery simultaneously with the field measurements on July 22 (Välisuo) and July 24 (Matorovansuo), 2023, using a DJI Matrice 300 RTK. The weather conditions during and between the flights were evenly cloudy and stable. The UAV imagery consisted of multispectral, thermal and topographic data, the former two of which were acquired using the MicaSense Altum-PT

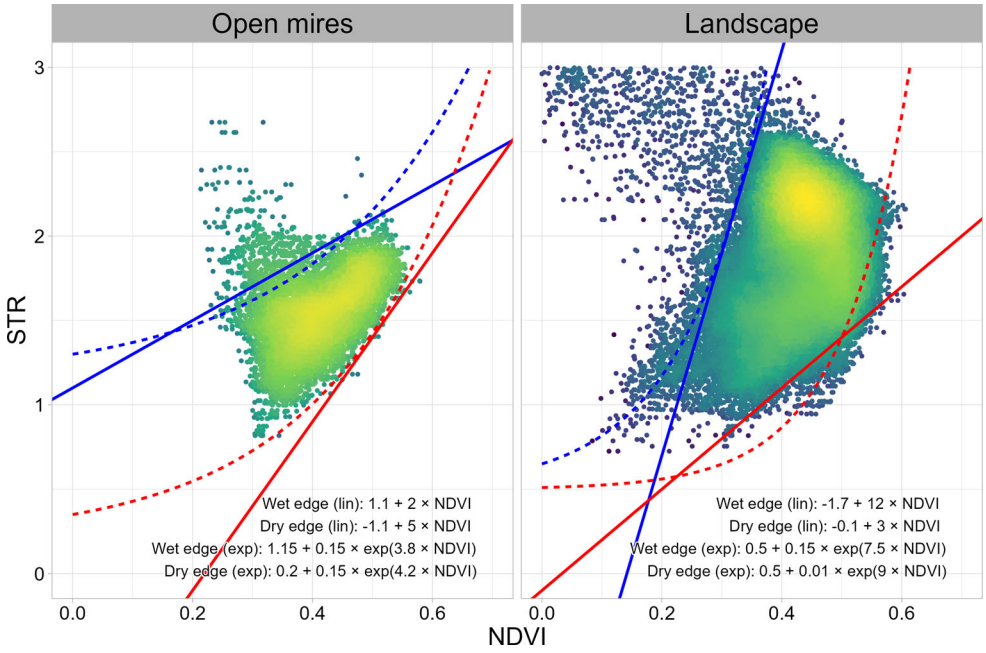

Fig. 2 The parameterization of OPTRAM from the density scatterplot in log2-sacle between the vegetation index NDVI and the shortwave infrared transformed reflectance (STR). We tested the parameterization with linear and exponential wet and dry edges for two different geographical area delineations: open mire area and larger landscape area consisting of also forests on mineral and peat soil. For the landscape area delineation, oversaturated pixels with STR > 3 or NDVI < 0 are not shown in the figure and they were not considered in the parameterization

sensor and the latter using YellowScan's Mapper+ sensor. The multispectral and thermal surveys had a flight altitude of 120 m, a side overlap of 75%, a front overlap of 70% and a flight speed of 9 m/s. The spatial resolution was ca. 5 cm and ca. 30 cm for the multispectral and thermal imagery, respectively. Radiometric consistency of the multispectral data was improved by using the built-in irradiance sensor of the MicaSense Altum-PT to account for changing light conditions during the flight. A calibration panel with known reflectance values was photographed before and after each mission to support reflectance correction. The multispectral imagery was then converted to normalized reflectance values using both the panel measurements and the irradiance data. Real-time positioning corrections were obtained through the VRS network to improve geolocation accuracy. The UAV lidar surveys had a flight altitude of 100 m, a side overlap of 55%, and a flight speed of 7 m/s in Välisuo and 8 m/s in Matorovansuo. The resultant spatial resolution of the topographic data was 20 cm.

The satellite imagery used was openly available Sentinel-2 imagery produced by the European Space Agency (ESA). We selected a cloud-free image acquired on July 12 with preprocessing level 2A. From the imagery, we utilized visible and near-infrared bands with original spatial resolution of 10 m as well as red edge and shortwave infrared bands with original spatial resolution of 20 m. We resampled the 20 m spatial resolution bands into 10 m spatial resolution using the nearest neighbor method. The chosen image was from a date as close as possible to the UAV imagery and field measurements, with temporal gap being 10–13 days.

We calculated NDVI and STR from the Sentinel-2 satellite imagery to construct a scatterplot, for which we tested four different parameterization options to depict the OPTRAM wet and dry edges (Fig. 2). We tested two different methods for delineating the edges: traditional linear lines (Sadeghi et al. 2017) and exponentially fitted curves that have been shown to delineate the wet and dry edges more accurately in some cases (Ambrosone et al. 2020). Further, as it has been shown that the delineation of geographical area used in OPTRAM parameterization matters (Mohamadzadeh et al. 2025), we tested fitting both linear and exponential versions of OPTRAM for two different geographical areas: (i) open mire area delineation (Fig. 1), (ii) larger 5 × 5 km landscape area around the study sites consisting of open mires as well as forests on mineral and peat soil. We fitted the lines visually since that has shown to be a good approach (Sadeghi et al. 2017). When positioning the lines, we aimed to include the majority of the points inside the trapezoid, apart from excluding sparse points above the wet edge or below the dry edge. When fitting the edges for the larger landscape area, we did not consider pixels located in open water bodies and other oversaturated areas (NDVI < 0 or STR > 3). To calculate OPTRAM, the wet and dry edge parameters were placed in the formulas indicated in Table 1.

In addition to OPTRAM, we calculated several other hydrological and vegetation indices from the Sentinel-2 and UAV imagery (Table 1). We chose indices utilized in earlier studies in peatlands similar to our study sites (Isoaho et al. 2024a, b; Räsänen et al. 2022). We calculated the Thermal-Optical Trapezoid Model (TOTRAM, Sadeghi et al. 2017) by delineating the wet and dry edges linearly using the open

Table 1 The bands and indices calculated from Sentinel-2 and uncrewed aerial vehicle imagery (UAV)

	Abbreviation	Name	Equation	Reference	Sentinel-2	UAV
Single bands	Blue	Blue reflectance	N/A	N/A	x	x
	Green	Green reflectance	N/A	N/A	x	x
	Red	Red reflectance	N/A	N/A	x	x
	RE	Red edge reflectance	N/A	N/A	x	x
	RE2	Red edge 2 reflectance	N/A	N/A	x	–
	RE3	Red edge 3 reflectance	N/A	N/A	x	–
	NIR	Near-infrared reflectance	N/A	N/A	x	x
	SWIR1	Shortwave infrared 1 reflectance	N/A	N/A	x	–
	SWIR2	Shortwave infrared 2 reflectance	N/A	N/A	x	–
Vegetation indices	NDVI	Normalized Difference Vegetation Index	$\frac{NIR-Red}{NIR+Red}$	(Tucker 1979)	x	x
	GDVI	Green Difference Vegetation Index	$NIR - Green$	(Sripada et al. 2006)	x	x
	EVI	Enhanced Vegetation Index	$2.5 * \frac{NIR-Red}{NIR+6*Red-7.5*Blue+1}$	(Huete et al. 1997)	x	x
	SAVI	Soil Adjusted Vegetation Index	$1.5 * \frac{NIR-Red}{NIR+Red+0.5}$	(Huete et al. 1997)	x	x
	NDRE	Normalized Difference Red Edge Index	$\frac{NIR-RedEdge}{NIR+RedEdge}$	(Sims and Gamon 2002)	x	x
	NDRE2	Normalized Difference Red Edge Index 2	$\frac{NIR-RedEdge2}{NIR+RedEdge2}$	(Sims and Gamon 2002)	x	–
	NDRE3	Normalized Difference Red Edge Index 3	$\frac{NIR-RedEdge3}{NIR+RedEdge3}$	(Sims and Gamon 2002)	x	–
Hydrological indices	STR	Shortwave infrared transformed reflectance	$\frac{(1-SWIR2)^2}{2SWIR2}$	(Sadeghi et al. 2017)	x	–
	$OPTRAM_{lin}$	Optical Trapezoid Model; linear fit	$\frac{STR-(i_d+s_d NDVI)}{(i_w+s_w NDVI)-(i_d+s_d NDVI)}$	(Sadeghi et al. 2017)	x	–
	$OPTRAM_{exp}$	Optical Trapezoid Model; exponential fit	$\frac{STR-(i_d+s_{d,1}e^{s_{d,2}NDVI})}{(i_w+s_{w,1}e^{s_{w,2}NDVI})-(i_d+s_{d,1}e^{s_{d,2}NDVI})}$	(Ambrosone et al. 2020)	x	–
	TOTRAM	Thermal-Optical Trapezoid Model	$\frac{LST-(i_d+s_d NDVI)}{(i_w+s_w NDVI)-(i_d+s_d NDVI)}$	(Sadeghi et al. 2017)	–	x
	NDMI1	Normalized Difference Moisture Index 1	$\frac{NIR-SWIR1}{NIR+SWIR1}$	(Gao et al. 1996)	x	–
	NDMI2	Normalized Difference Moisture Index 2	$\frac{NIR-SWIR2}{NIR+SWIR2}$	(Gao et al. 1996)	x	–
	NDWI	Normalized Difference Water Index	$\frac{Green-NIR}{Green+NIR}$	(McFeeters 1996)	x	x
	SWI	Saga Wetness Index	$\ln(\frac{A_{SM}}{tan\beta})$	(Böhner and Selige 2002)	–	x

Abbreviations in equations: i_d intercept of the dry edge, i_w intercept of the wet edge, s_d slope of the dry edge, s_w slope of the wet edge, A_{SM} specific catchment area, β local slope
Note that for exponentially fitted OPTRAMs, there are two slope constants, numbered 1 and 2

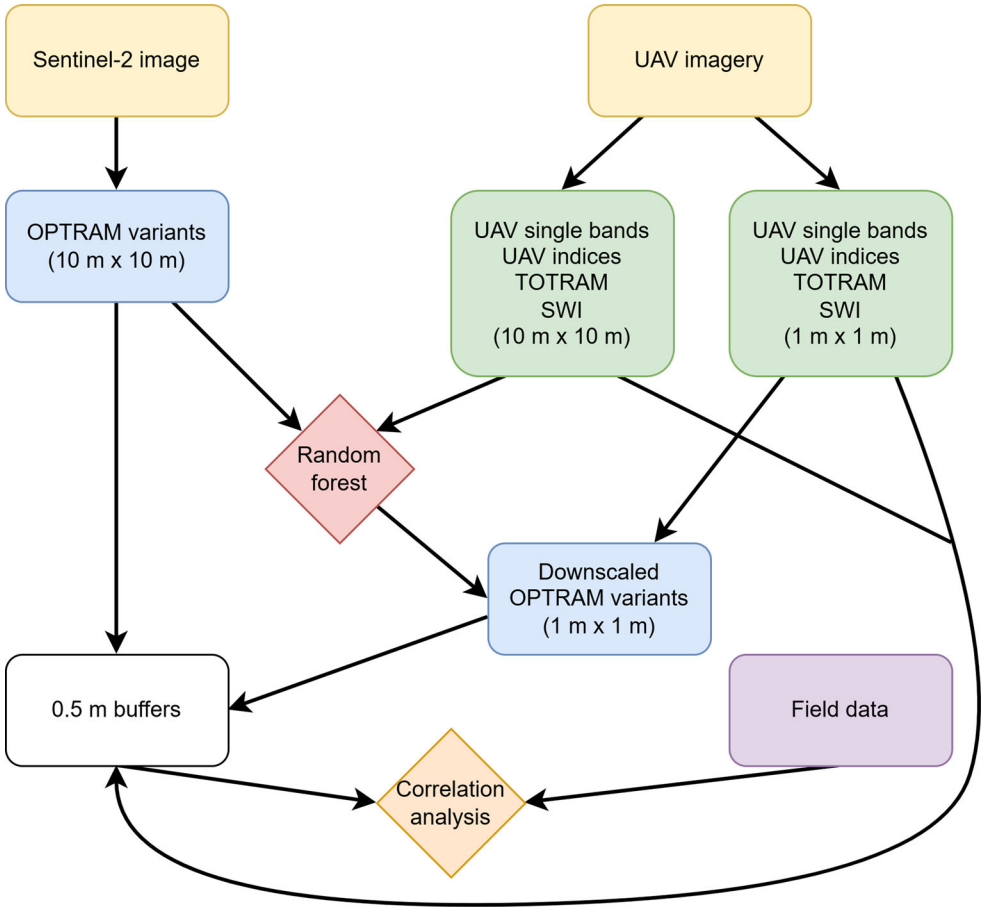

Fig. 3 The workflow of the used materials and methods

mire area delineation from the scatterplot between NDVI and land surface temperature (LST) attained from the UAV imagery. We derived the LST from Altum-PT's calibrated thermal infrared band with MicaSense's formula ("Altum and Altum-PT Thermal Band—FAQ" 2023). We calculated the indices using R (version 4.4.1) apart for SWI which we determined with SAGA GIS using the parameters presented by Ikkala et al. (2022).

2.3 Downscaling and Other Analysis Methods

We manually delineated the open areas of the studied peatlands and used that delineation (Fig. 1) to construct a 10 m × 10 m grid to match the satellite imagery's pixel size and spacing (Fig. 3). We then calculated mean values for the UAV variables for each grid cell, spatially weighted by the fraction that each pixel covers the grid cell. In addition, we joined the OPTRAM values to the grid cells. To downscale OPTRAM, we constructed a second grid with a 1 m × 1 m cell size using the same open area delineation and calculated spatially weighted mean values of the UAV variables for its cells.

We trained random forest regression models using data from the 10 m × 10 m grid, with the OPTRAM variants as the response variables and the weighted mean values of UAV variables as predictors. We chose random forest due to its ability to handle multicollinear predictors and non-linear relationships between predictors and response variable (He et al. 2016), as well as to not overfit (Breiman 2001).

Before implementing the models, we tested variable selection with Variable Selection Using Random Forest (VSURF; Genuer et al. 2015). However, it indicated that all variables were important for the models; thus, we included all UAV variables as predictors.

We set the number of decision trees at 500, since any number of trees over 100 seems to achieve a robust performance level (Probst et al. 2019; Rodriguez-Galiano et al. 2012). We used the default value of predictors tested at each tree node (1/3 of predictors) due to its high previous performance (e.g. Isoaho et al. 2024b). To evaluate the success of OPTRAM's downscaling, we validated the models using 10-fold spatial block cross-validation in which we divided the study area into 250 m × 250 m blocks which we randomly placed into each fold.

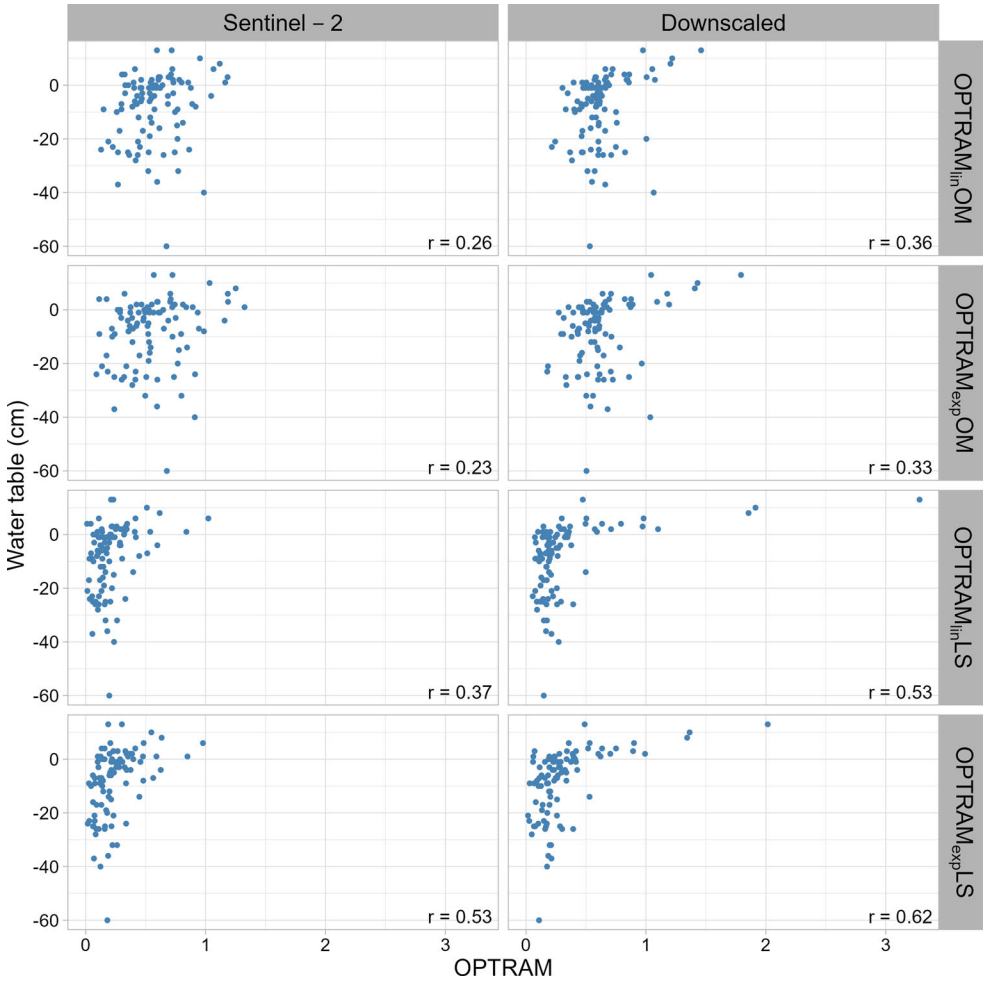

Fig. 4 The scatterplots between WT and the original Sentinel-2 OPTRAMs (left panel) and OPTRAMs downscaled with UAV variables (right panel). The results are shown for all four OPTRAM parameterizations (linear and exponential fits, separately for open mire (OM) and landscape (LS) delineation). r stands for the Spearman correlation coefficient

To evaluate model performance, we calculated the Root Mean Squared Error and the percentage of explained variance which was calculated as:

$$1 - \frac{MSE}{var\,(y)} \times 100,$$

where *var(y)* is the variance of the response variable. Using the random forest models, we predicted OPTRAM pixel values for the 1 m × 1 m grid.

Moreover, we collected the importance values of the predictors using permutation importance. We normalized the importance values between 0–100 with their sum being 100 to ease the comparison between predictors.

Lastly, we collected values of the downscaled and original OPTRAMs as well as the other Sentinel-2 and UAV variables to buffers with a radius of 0.5 m and centers located at the field measurement points. We calculated correlations between WT and the variables in the buffers using the Spearman correlation coefficient (r_s) due to its ability to handle nonlinear correlations.

3 Results

3.1 OPTRAM Parameterization

The OPTRAM-WT correlation was heavily dependent on OPTRAM parameterization, with r_s ranging from 0.23 to 0.53 (Fig. 4). The correlations were higher when dry and wet edges were parameterized with landscape delineation than using the open mire area delineation. The highest OPTRAM-WT correlation was obtained when the dry and wet edges were exponentially fitted from the landscape-level delineation, while the lowest correlation was obtained also with exponentially fitted dry and wet edges but open mire area delineation.

3.2 OPTRAM Downscaling

Downscaling OPTRAM with UAV variables and random forest model increased the OPTRAM-WT correlation by 0.09 to 0.16 units, up to $r_s = 0.62$ for the best performing parameterization (Fig. 4). The random forest models achieved explained variance of 45.6–72.4%, with the most important

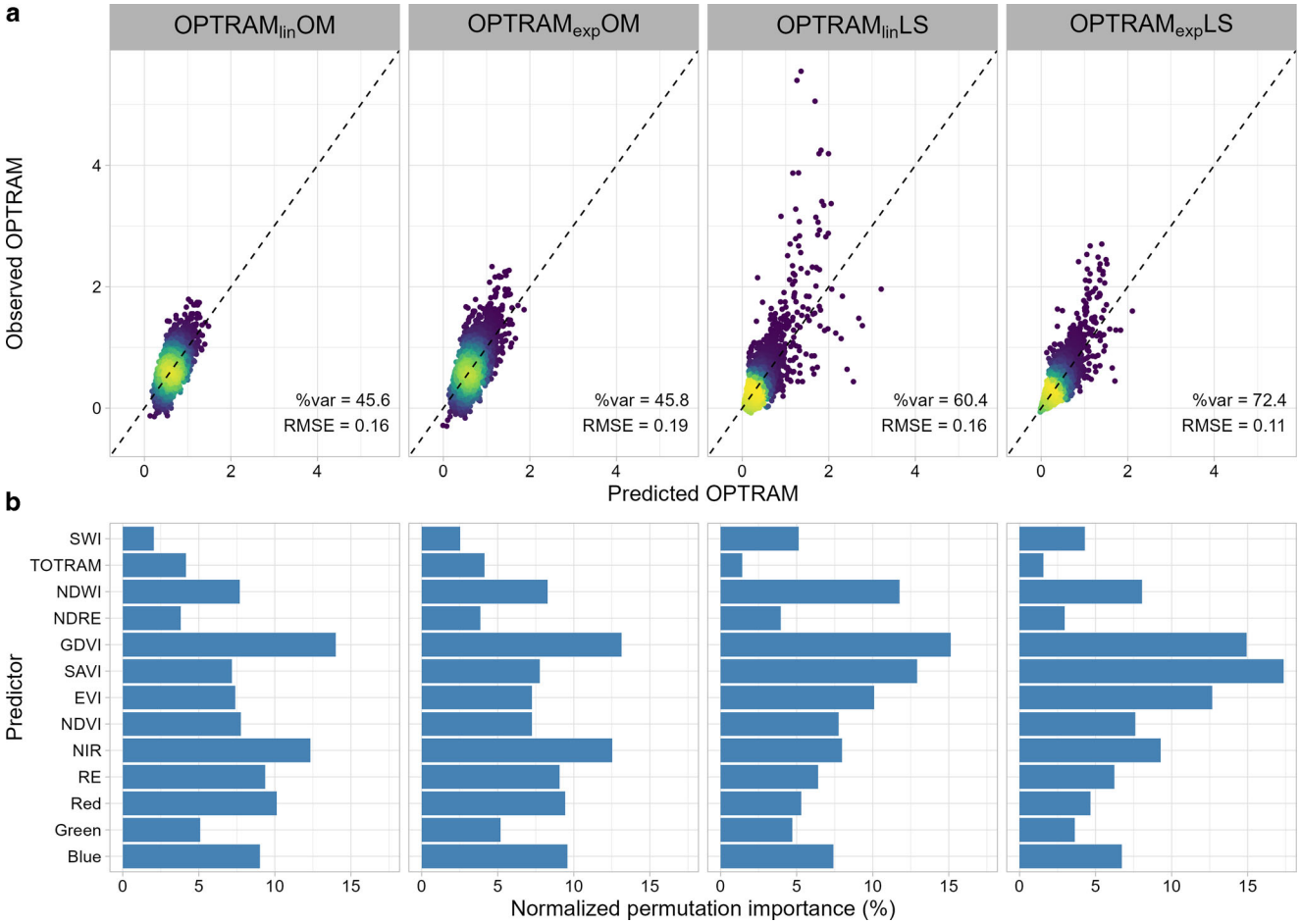

Fig. 5 The observed-predicted density scatterplots of the random forest models used in OPTRAM downscaling (**a**) and the most important predictors in each model (**b**). The results are shown for all four OPTRAM parameterizations (linear and exponential fits, separately for open mire (OM) and landscape (LS) delineation). %var refers to percentage of explained variance and RMSE to Root Mean Squared Error. Other abbreviations are explained in Table 1

predictors being mostly vegetation greenness indices and NIR reflectance (Fig. 5). The connection between the downscaled OPTRAMs and WT was more regular compared to the original OPTRAMs, as there was less dispersion in the downscaled OPTRAM-WT scatterplots (Fig. 4). Furthermore, the spatial distributions of the original and downscaled OPTRAMs differed significantly when inspected visually (Fig. 6). The downscaled OPTRAMs revealed the fine-resolution variation of WT in the flark-string pattern at both study sites realistically while the original OPTRAMs could differentiate only the coarser spatial-scale patterns in WT. The spatial patterns of OPTRAM values were relatively similar between the four different parameterization options but the OPTRAMs with a higher WT correlation could differentiate the high and low WT areas more distinctly.

3.3 Correlations Between the Other Remote Sensing Variables and Water Table

The correlations between the UAV variables and WT varied notably (Fig. 7a). NDVI and NDWI achieved the strongest correlations ($r_s = -0.66$ and $r_s = 0.67$, respectively). EVI and SAVI correlated almost as strongly ($r_s = -0.65$). Among the single band variables, near infrared achieved the strongest correlation ($r_s = -0.56$) and green the lowest ($r_s = -0.14$). TOTRAM showed the lowest correlation ($r_s = -0.09$) while topography based SWI had a correlation on par with the best performing downscaled OPTRAM ($r = 0.62$).

Similar trends could be seen in the correlations between Sentinel-2 variables and WT. The highest correlations were obtained for NDVI, NDWI, EVI, SAVI and NDRE1 ($|r_s| = 0.57–0.58$), followed by GDVI and NDMI2. Of the single bands, the highest correlation was for NIR, RE2, and RE3 while the correlation was notably weak for SWIR and green bands.

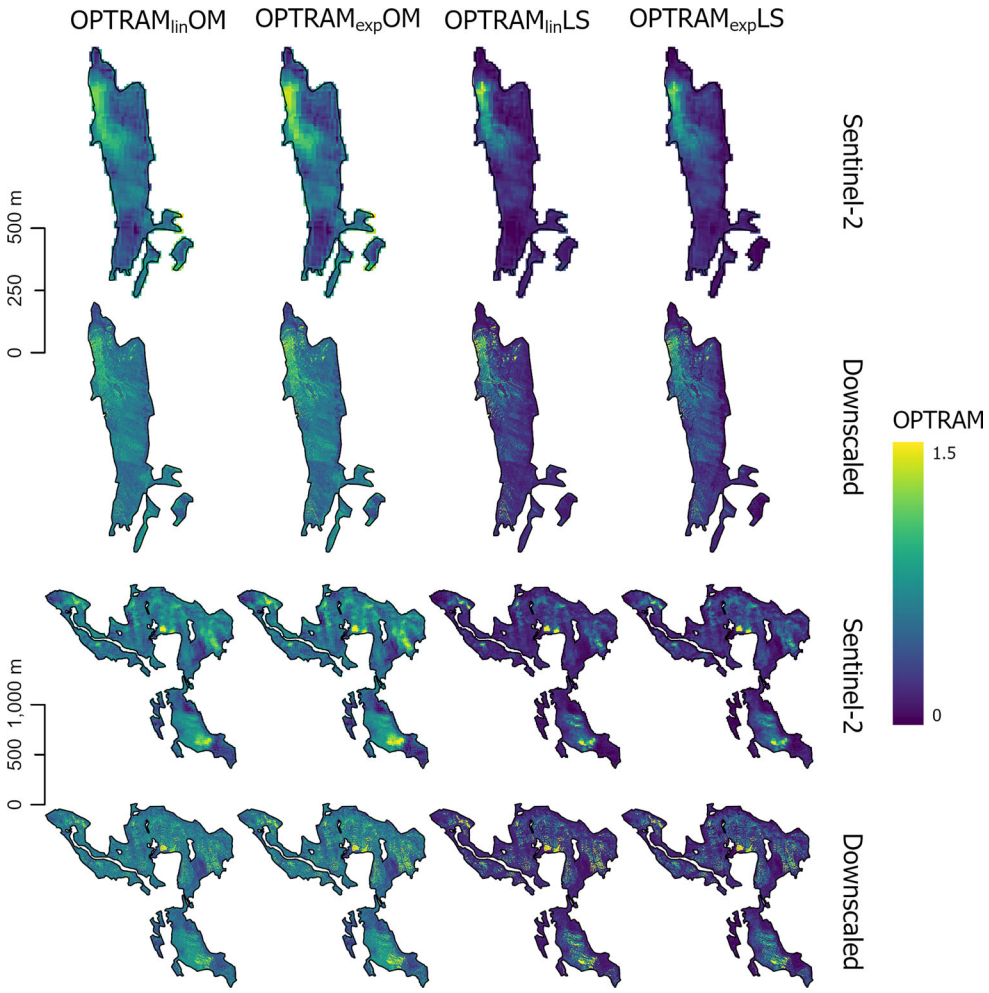

Fig. 6 Spatial distributions of the original and downscaled OPTRAMs in the study sites Välisuo (top panel) and Matorovansuo (bottom panel). The maps are shown for all four OPTRAM parameterizations (linear and exponential fits, separately for open mire (OM) and landscape (LS) delineation)

4 Discussion

4.1 OPTRAM Parameterization

The OPTRAM-WT correlation was highly dependent on OPTRAM parameterization. Surprisingly, we obtained the highest correlations when delineating the dry and wet edges with satellite imagery clipped to a larger mosaic landscape area, even though Mohamadzadeh et al. (2025) have shown that land cover type specific OPTRAM parameterization improves its performance. The larger landscape area delineation consisted of pixels from different types of ecosystems and land cover than our focal open mire study area. These included densely treed forests in which Sentinel-2 surface reflectance observations are mostly from top of the canopy and not from peatland surface. One reason behind this surprising result might be that our open mire area delineation included ca. 13,000 Sentinel-2 pixels which is half of the 25,000-pixel threshold that Burdun et al. (2023) considered to be minimum for reliable wet and dry edge delineation. Nevertheless, in our case, also for the open mire area delineation, the wet and dry edges could be interpreted from the NDVI-STR scatterplot.

We received mixed evidence whether exponentially fitted dry and wet edges (c.f. Ambrosone et al. 2020) improve OPTRAM performance in WT modeling: with open mire delineation, exponentially fitted OPTRAM performed worse than the traditional linearly fitted OPTRAM while the situation was the opposite when we conducted OPTRAM parameterization using a larger landscape area delineation. Indeed, we obtained the highest OPTRAM-WT correlation with the OPTRAM parameterized with exponentially fitted dry and wet edges and data from a larger landscape area, possibly suggesting the benefits of exponentially fitting wet and dry edges.

OPTRAM parameterization affected OPTRAM-NDVI and OPTRAM-STR correlations, with the OPTRAM-NDVI correlation strengthening from –0.35 to –0.90 and OPTRAM-STR correlation weakening from 0.56 to –0.13 when the OPTRAM-WT correlation increased. This result is in line with the fact that NDVI-WT correlation was notably higher than STR-WT correlation while OPTRAM-WT correlation was in between these two correlations.

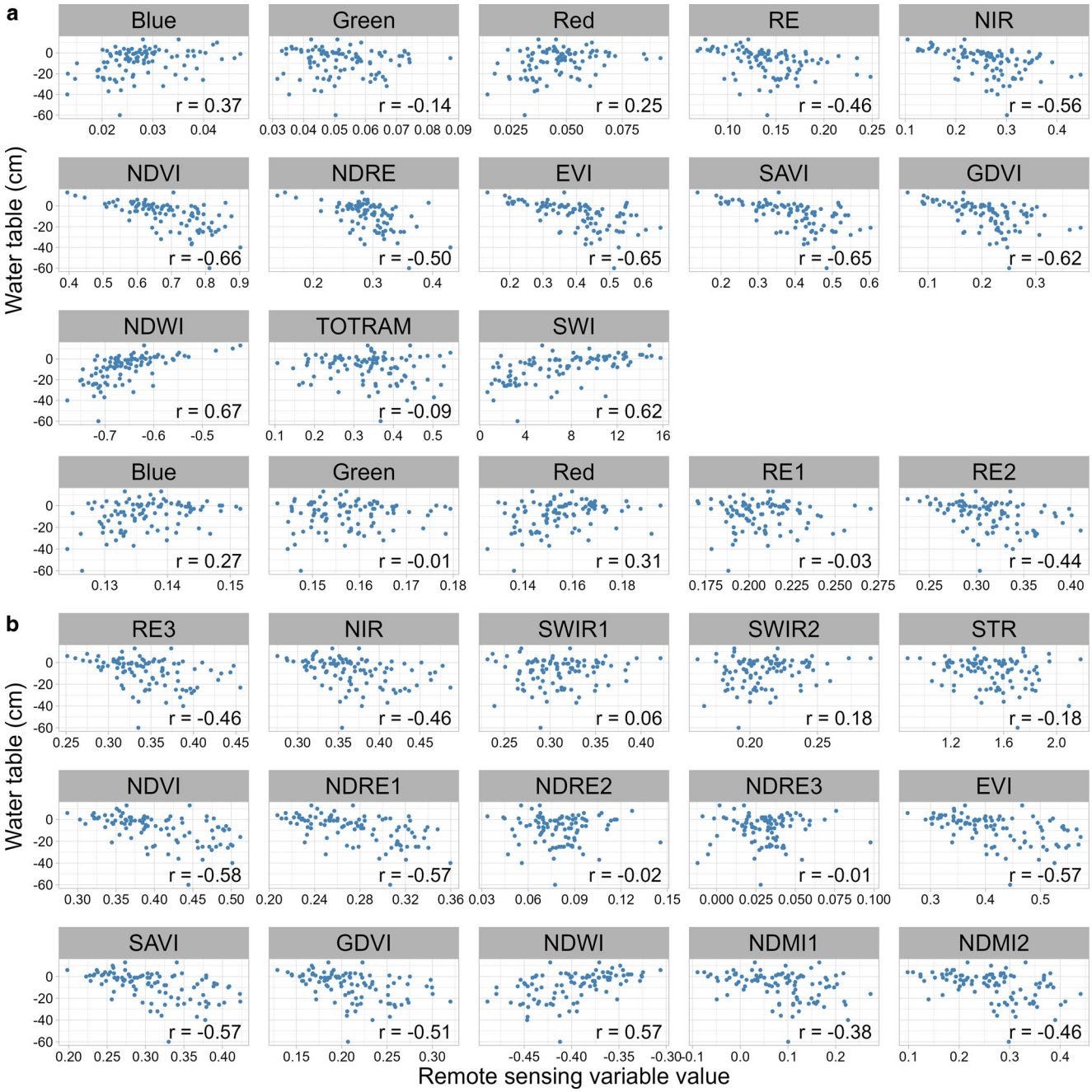

Fig. 7 Scatterplots and Spearman correlation coefficients between WT and uncrewed aerial vehicle variables (**a**), and Sentinel-2 variables (**b**). The abbreviations are explained in Table 1

Therefore, with OPTRAM parameterization, the relative role of NDVI versus STR can be adjusted. Nevertheless, a more important question is why NDVI was a better proxy to model peatland WT than STR, OPTRAM, or other SWIR-based variables in our study. Indeed, earlier studies focusing on temporal and spatiotemporal monitoring of peatland WT have highlighted the importance of SWIR reflectance (Räsänen et al. 2022; Isoaho et al. 2024b; Reddin et al. 2025) and have identified OPTRAM highly promising in the monitoring of WT and restoration effects in open peatlands (Burdun et al. 2020, 2023; Räsänen et al. 2022).

NDVI is linked to the amount of green vegetation (Tucker 1979), and in our study sites, there is a notable variation in the amount of green vegetation between vegetated dry strings and largely non-vegetated wet flarks that are partly covered by shallow water. The amount of vegetation is thus closely linked to the relative WT, with WT being deepest in strings and shallowest or even above

the ground in flarks. Therefore, our results suggest that in aapa mires with a clear string-flark pattern, vegetation greenness proxies are related to spatial variation of WT. Nevertheless, in other types of peatlands or ecosystems, the spatial patterns of WT can possibly be explained by other proxies; for instance, it has been shown that the temporal NDVI-WT correlation can range from highly negative to highly positive (Burdun et al. 2023).

On balance, it might be that SWIR-based reflectance is better suited to temporal peatland WT monitoring (Räsänen et al. 2022; Burdun et al. 2023; Isoaho et al. 2024b; Reddin et al. 2025), instead of modeling spatial variation in patterned aapa mires. In peatland ecosystems, temporal variation in WT causes different types of changes in surface reflectance than spatial variation. Spatially, there is a large variation in land and surface cover from shallow open water to dense green shrub and other vascular vegetation cover. Temporally, within one location, the type of vegetation is relatively stable and also the wettest flark areas are covered by shallow water throughout the snow-free season. Even though there are phenological changes particularly in areas covered by deciduous vegetation, the temporal variation in reflectance is probably subtler than spatial variation. Furthermore, it might be that different remotely sensed signals are better to depict temporal variation in WT than spatial patterns in it. As there is also a high between-site variability in the most important remote sensing variables explaining WT variation (Räsänen et al. 2022), further research is needed to analyze which variables are linked to spatial and which to temporal WT variation in different peatland sites. As a part of this work, OPTRAM and its different parameterization options should be tested.

Our study sites were partly drained when we conducted the research. After our field work, the sites were restored by filling drainage ditches and directing water to undrained open mire areas. Earlier studies have indicated that OPTRAM's ability to indicate WT is decreased in drained and dry peatlands with WT deep below the ground level (Burdun et al. 2023; Räsänen et al. 2022). In case OPTRAM's weak connection to WT is caused by drying, it could in turn allude to test OPTRAM's potential in restoration monitoring, also in our study sites. After restoration, peatland WT rises (Haapalehto et al. 2014; Menberu et al. 2016), possibly resulting in a strengthened connection between OPTRAM and WT.

4.2 OPTRAM Downscaling

We noticed an improvement in the connection between OPTRAM and WT after downscaling, as the correlation strengthened by 0.09–0.16 units, and the spatial result was more precise in visualizing the flark-string pattern and small-scale spatial variation in WT. Differentiating the small-scale spatial patterns in WT has been noted as an essential but challenging aspect of peatland remote sensing because peatlands are spatially highly heterogeneous ecosystems (Ikkala et al. 2022; Isoaho et al. 2023; Jussila et al. 2024; Steenvoorden and Limpens 2023). Therefore, the results imply that downscaling with UAV data could respond to the requirement of peatland WT monitoring: downscaling facilitates combining high spatial resolution UAV data with high temporal resolution and large spatial extent satellite data. Multitemporal satellite imagery could even be downscaled with a snapshot UAV image if high-spatial resolution patterns of WT remain relatively stable over time and temporal changes are more evident in coarser spatial resolutions.

The downscaling of soil moisture can be thought of being an opposite way to achieve field data for a remote sensing-based model. Field data is normally used to upscale moisture across the peatland (e.g. Isoaho et al. 2024b; Reddin et al. 2025), but with downscaling, the moisture data is collected from a coarser resolution product and then scaled to reflect the spatial heterogeneity in the field and possibly validated with field reference data (e.g. Jääskeläinen et al. 2025). The usability of downscaling and combining UAV and satellite data in peatland monitoring is further encouraged, since UAV data is unlikely to reach the level of temporal and geographical coverage of satellites (Jussila et al. 2024; Lendzioch et al. 2021; Steenvoorden et al. 2023).

The random forest used for upscaling was successful with all four OPTRAM parameterization options. The relatively good performance was partly expected due to the downscaling of soil moisture with random forest yielding good results earlier (Fu et al. 2024; Im 2016; Mahmood 2024; Jääskeläinen et al. 2025). Nevertheless, the spatial resolution here is largely different from previous studies as they have utilized kilometer-resolution datasets for downscaling, while we utilized meter-resolution datasets. All used UAV variable types produced important variables for the downscaling model. Optical, topographical, and thermal imagery have all performed well in earlier soil moisture and WT studies, although thermal imagery has acted a more important role compared to our results (Abowarda 2021; Fu et al. 2024; Im 2016). The difference could be explained by differing spatial resolution, but also differing target ecosystems, since earlier downscaling studies have not focused on northern peatlands, in which results have deviated from the general connection between soil temperature and moisture (Burdun et al. 2020).

Leveraging random forest in downscaling seems to be recommendable in light of our results and previous studies. The method has multiple advantages, such as ease of use, ability to handle multicollinear variables and tendency not to overfit. However, some limitations arise in its application to hydrological peatland studies. First, the performance of

random forest models depicting hydrological characteristics of peatlands vary between sites (e.g. Lendzioch et al. 2021; Räsänen et al. 2022), alluding to restricted possibilities of generalization. However, the inability to generalize is not restricted to random forest, but rather a common issue in machine learning. Second, random forest underestimates extreme values in regression applications (He et al. 2016), which may impair OPTRAM's prediction performance in flarks and other areas of high WT. It could be beneficial to test alternate machine learning methods, such as the Light Gradient-Boosting Machine developed by Ke et al. (2017), which yielded good results when downscaling soil moisture in boreal forests (Jääskeläinen et al. 2025). Additionally, deep learning methods could produce improved results compared to traditional machine learning (Foroumandi 2023; Rezaee 2018).

Although the use of OPTRAM and downscaling require more steps compared to downscaling single bands or indices, using downscaled OPTRAM could be worthwhile when monitoring peatland WT even without ground reference data. Burdun et al. (2023) and Karlqvist et al. (2024) have noticed that OPTRAM's ability to monitor peatland WT and *Sphagnum* moisture content, respectively, is stabler than that of spectral indices, which increases OPTRAM's potential for acting as a WT proxy, particularly in cases with limited field data and in multi-site peatland studies. However, as OPTRAM needs separate parameterization in different study sites (Sadeghi et al. 2017), in studies with a large number of study sites, OPTRAM parameterization should be automatized to avoid laborious manual parameterization. Previously, the automatization of OPTRAM's parametrization has been challenging in small peatland areas but promising otherwise (Burdun et al. 2023), alluding to an improved efficiency of applying OPTRAM to larger amounts of study sites and data.

4.3 Connections of Other Remote Sensing Variables to Water Table

The downscaled OPTRAM with the highest correlation had almost as high correlation (r = 0.62) with WT than the highest-correlating UAV variable NDWI (r = 0.67). In general, most variables present in both UAV and Sentinel-2 showed correlation increases with higher spatial resolution, and similar increase was achieved with the downscaled OPTRAMs. Correlation differences furthermore suggest that, in our study sites, Sentinel-2 data suffers from a mixed pixel problem and is too coarse to observe fine-spatial resolution variation in WT. The mixed pixel problem is also more severe for RE and SWIR bands due to their lower spatial resolution (20 m) compared to the rest of the bands (10 m). However, most of the RE bands had relatively similar correlations with WT compared to NIR while SWIR bands had the lowest correlations.

Overall, for both UAV and Sentinel-2 imagery, the strongest correlations with WT were reached by different optical indices. The good performance of optical variables is in line with results from earlier studies (e.g. Isoaho et al. 2023, 2024b; Jussila et al. 2024; Lendzioch et al. 2021; Räsänen et al. 2022). The strongest correlations included vegetation greenness and water indices, which supports earlier observations of connections of both vegetation and water with peatland WT (Irfan et al. 2020; Kolari et al. 2021; Potvin et al. 2015). Even so, strongly correlated NDWI has not acted as a significant indicator of peatland WT earlier (Isoaho et al. 2024b; Räsänen et al. 2022); however, its value in our case can be explained by the study area which includes wet flarks with shallow open water. Furthermore, NDWI-NDVI correlation was close to –1 suggesting that NDWI gives almost similar information to NDVI that is used in OPTRAM parameterization.

Single bands performed weaker than indices, except for NIR and some of the RE bands which correlated moderately with WT. Of these, NIR has been found to be a good proxy for peatland wetness in earlier studies (Kolari et al. 2022; Isoaho et al. 2023). Single bands have in some cases outperformed indices calling into question the necessity of indices (Isoaho et al. 2024b; Kolari et al. 2022), but in contrast, our results support their usefulness.

Thermal variables have been well-functioning proxies for peatland WT previously (Isoaho et al. 2023; Lendzioch et al. 2021). Nevertheless, thermal-based TOTRAM did not correlate strongly with WT in our results. Therefore, TOTRAM does not seem to have that strong a connection with WT in northern peatlands which has been suggested also previously (Burdun et al. 2020). TOTRAM's otherwise good performance in hydrological studies conducted elsewhere than in northern peatlands might be due to the wetness and lack of energy available to vegetation (Burdun et al. 2020). The dates when UAV flights were conducted, were consistently cloudy which prevented the sun from warming non-wet surfaces more than wet surfaces. As the relationship between LST and wetness is the main assumption of TOTRAM (Sadeghi et al. 2017), this partly explains its low importance to the downscaling models and low correlation with WT. Furthermore, the low TOTRAM-WT correlation could also be explained by parameterization; while we tested several parameterization options for OPTRAM, we relied on one parameterization for TOTRAM. Nonetheless, TOTRAM had a weaker correlation with WT than any of the OPTRAM variants.

The topographic variable SWI had a correlation with WT on par with the highest correlating downscaled OPTRAM. Previously, SWI's performance has yielded varying results in WT and moisture monitoring (Ikkala et al. 2022; Isoaho

et al. 2023; Kemppinen et al. 2018; Kopecký et al. 2021). SWI's feasibility is supported by deriving it from high spatial resolution lidar data, allowing the observation of small-scale wetness variability (Ikkala et al. 2022; Kemppinen et al. 2018). Using SWI in WT monitoring is further supported by its suitability to flat study areas in comparison to other topographic indices (Mattivi et al. 2019).

4.4 Possible Sources of Uncertainty

There are some uncertainties caused by data quality. First, we could not attain cloud-free satellite imagery for the time of field measurements and UAV flights. Instead, there was a 10–13-day gap between the satellite imagery and other data. During this period, the cumulative rainfall was ca. 50 mm in the weather station (Kittilä Kenttärova) located in between the two study sites, possibly causing differences in the hydrological conditions and affecting the connection between the satellite-derived OPTRAM and the field-measured WT. Additionally, similar conditions during field measurements and UAV flights could play a role in the strong connections between the UAV variables and WT. However, the temporal gap is small and the uncertainty it causes is likely not large, particularly since all data were collected during the peak growing season in middle to late July. Second, the field measurement method holds some uncertainty. Representative measurements may not have been achieved from all pipes due to WT possibly not rising inside the pipe to the same level as in the surrounding area.

Third, some uncertainty is caused by OPTRAM's visual parameterization even though the visual fitting of the wet and dry edges is recommended and preferred to statistical options (Sadeghi et al., 2017). We managed this uncertainty by testing four different parameterization options, but other parameterization approaches could have been tested as well. Fourth, since OPTRAM has originally been developed to detect soil moisture, it might not be suitable for predicting WT above the ground level. This creates uncertainty in wet flarks where OPTRAM's prediction capabilities can be limited. It might be recommendable to delineate study sites to areas with WT belowground or alternatively use different methods. One such alternative could be the newer version of OPTRAM which aims to correct the issue of oversaturation by adjusting OPTRAM values for the pixels located above the wet edge (Sadeghi et al. 2023). Alternatively, Burdun et al. (2023) used additional methods with visual parameterization to filter oversaturated pixels from their data, which could have improved OPTRAM's connection to WT by diminishing the effect of highly saturated pixels.

5 Conclusions

We have tested the performance of OPTRAM downscaled with UAV variables in detecting spatial patterns of WT in northern peatlands. Our results suggest that OPTRAM parameterization matters, downscaling strengthens the connection between OPTRAM and WT, and downscaled OPTRAM can have nearly as high correlation with WT than the best performing UAV variables. Downscaling enables the detection of small-scale spatial WT variation and can provide a way of combining satellite and UAV imagery to allow for high resolution spatiotemporal WT monitoring. Furthermore, our results encourage the use of downscaling methods at high spatial resolutions, as well as integrating multi-sensor and machine learning methods in peatland WT monitoring.

Supplementary Information The online version of this article (https://doi.org/10.1007/s41064-026-00389-8) contains supplementary material, which is available to authorized users.

Acknowledgements We thank Kaapro Keränen for assistance in the field work. The work was funded by the Ministry of the Environment, Finland (grant no. VN/14352/2022) and European Union Life Programme (LIFE21-CCM-LV-LIFE-PeatCarbon; LIFE22-IPN-FI-Priodiversity LIFE).

Author contributions A.I., A.R and S.H. designed the study. S.H. conducted the analyses under supervision by A.I. and A.R. A.K., P.K., and T.K. provided the uncrewed aerial vehicle data. S.H. wrote the first draft of the manuscript. All authors reviewed the manuscript.

Funding Open Access funding provided by University of Oulu (including Oulu University Hospital).

Data Availability A data table including plot coordinates, water table measurements, and remote sensing variables is provided within the supplementary material.

Competing interests The authors declare no competing interests.

References

Abowarda AS (2021) Generating surface soil moisture at 30 m spatial resolution using both data fusion and machine learning toward better water resources management at the field scale. Remote Sens Environ 255:112301. https://doi.org/10.1016/j.rse.2021.112301

Alm J, Wall A, Myllykangas J-P, Ojanen P, Heikkinen J, Henttonen HM, Laiho R, Minkkinen K, Tuomainen T, Mikola J (2023) A new method for estimating carbon dioxide emissions from drained peatland forest soils for the greenhouse gas inventory of Finland. Biogeosciences 20:3827–3855. https://doi.org/10.5194/bg-20-3827-2023

Ambrosone M, Matese A, Di Gennaro SF, Gioli B, Tudoroiu M, Genesio L, Miglietta F, Baronti S, Maienza A, Ungaro F, Toscano P (2020) Retrieving soil moisture in rainfed and irrigated fields using Sentinel-2 observations and a modified OPTRAM approach. Int J Appl Earth Obs Geoinformation 89:102113. https://doi.org/10.1016/j.jag.2020.102113

Atkinson PM (2013) Downscaling in remote sensing. Int J Appl Earth Obs Geoinformation 22:106–114. https://doi.org/10.1016/j.jag.2012.04.012

Babaeian E, Sadeghi M, Jones SB, Montzka C, Vereecken H, Tuller M (2019) Ground, proximal, and satellite remote sensing of soil moisture. Rev Geophys 57:530–616. https://doi.org/10.1029/2018RG000618

Böhner J, Selige T (2002) Spatial prediction of soil attributes using terrain analysis and climate regionalization. Gottinger Geograpihsche Abh 115

Breiman L (2001) Random forests. Mach Learn 45:5–32. https://doi.org/10.1023/A:1010933404324

Burdun I, Bechtold M, Sagris V, Komisarenko V, De Lannoy G, Mander Ü (2020) A comparison of three trapezoid models using optical and thermal satellite imagery for water table depth monitoring in Estonian bogs. Remote Sens 12:1980. https://doi.org/10.3390/rs12121980

Burdun I, Bechtold M, Aurela M, De Lannoy G, Desai AR, Humphreys E, Kareksela S, Komisarenko V, Liimatainen M, Marttila H, Minkkinen K, Nilsson MB, Ojanen P, Salko S-S, Tuittila E-S, Uuemaa E, Rautiainen M (2023) Hidden becomes clear: optical remote sensing of vegetation reveals water table dynamics in northern peatlands. Remote Sens Environ 296:113736. https://doi.org/10.1016/j.rse.2023.113736

Campbell JB, Wynne RH, Thomas VA (2023) Introduction to remote sensing, 6th edn. Guilford, New York

Foroumandi E (2023) Drought monitoring by downscaling GRACE-derived terrestrial water storage anomalies: a deep learning approach. J Hydrol 616:128838. https://doi.org/10.1016/j.jhydrol.2022.128838

Fu X, Zhang Y, Guo L, Lü H, Ding Y, Meng X, Qin Y, Wang Y, Xi B, Xu S, Xu P, Zhang G, Jiang X (2024) High resolution (1-km) surface soil moisture generation from SMAP SSM by considering its difference between freezing and thawing periods in the source region of the Yellow River. Agric For Meteorol 358:110263. https://doi.org/10.1016/j.agrformet.2024.110263

Gao B, NDWI—A normalized difference water index for remote sensing of vegetation liquid water from space, Remote Sensing of Environment, Volume 58, Issue 3,1996,Pages 257–266,ISSN 0034-4257, https://doi.org/10.1016/S0034-4257(96)00067-3

Genuer R, Poggi J-M, Tuleau-Malot C (2015) VSURF: an R package for variable selection using random forests. R J 7:19–33

Haapalehto T, Kotiaho JS, Matilainen R, Tahvanainen T (2014) The effects of long-term drainage and subsequent restoration on water table level and pore water chemistry in boreal peatlands. J Hydrol 519:1493–1505. https://doi.org/10.1016/j.jhydrol.2014.09.013

He X, Chaney NW, Schleiss M, Sheffield J (2016) Spatial downscaling of precipitation using adaptable random forests. Water Resour Res 52:8217–8237. https://doi.org/10.1002/2016WR019034

Huete AR, Liu H, van Leeuwen WJD (1997) The use of vegetation indices in forested regions: issues of linearity and saturation. In: 1997 IEEE International Geoscience and Remote Sensing Symposium Proceedings. Remote Sensing—A Scientific Vision for Sustainable Development IGARSS'97. IEEE International Geoscience and Remote Sensing Symposium Proceedings. Remote Sensing—A Scientific Vision for Sustainable Development, vol 4, pp 1966–1968 https://doi.org/10.1109/IGARSS.1997.609169

Ikkala L, Ronkanen A-K, Ilmonen J, Similä M, Rehell S, Kumpula T, Päkkilä L, Klöve B, Marttila H (2022) Unmanned aircraft system (UAS) structure-from-motion (SfM) for monitoring the changed flow paths and wetness in minerotrophic Peatland restoration. Remote Sens 14:3169. https://doi.org/10.3390/rs14133169

Im J (2016) Downscaling of AMSR-E soil moisture with MODIS products using machine learning approaches. Environ Earth Sci 75:1. https://doi.org/10.1007/s12665-016-5917-6

Irfan M, Kurniawati N, Ariani M, Sulaiman A, Iskandar I (2020) Study of groundwater level and its correlation to soil moisture on peatlands in South Sumatra. J Phys Conf Ser 1568:12028. https://doi.org/10.1088/1742-6596/1568/1/012028

Isoaho A, Ikkala L, Marttila H, Hjort J, Kumpula T, Korpelainen P, Räsänen A (2023) Spatial water table level modelling with multi-sensor unmanned aerial vehicle data in boreal aapa mires. Remote Sens Appl Soc Environ 32:101059. https://doi.org/10.1016/j.rsase.2023.101059

Isoaho A, Elo M, Marttila H, Rana P, Lensu A, Räsänen A (2024a) Monitoring changes in boreal peatland vegetation after restoration with optical satellite imagery. Sci Total Environ 957:177697. https://doi.org/10.1016/j.scitotenv.2024.177697

Isoaho A, Ikkala L, Päkkilä L, Marttila H, Kareksela S, Räsänen A (2024b) Multi-sensor satellite imagery reveals spatiotemporal changes in peatland water table after restoration. Remote Sens Environ 306:114144. https://doi.org/10.1016/j.rse.2024.114144

Jääskeläinen E, Luoto M, Putkiranta P, Aurela M, Virtanen T (2025) High-resolution soil moisture mapping in northern boreal forests using SMAP data and downscaling techniques. Hydrol Earth Syst Sci 29(21):6237–6256. https://doi.org/10.5194/hess-29-6237-2025

Jussila T, Heikkinen RK, Anttila S, Aapala K, Kervinen M, Aalto J, Vihervaara P (2024) Quantifying wetness variability in aapa mires with Sentinel-2: towards improved monitoring of an EU priority habitat. Remote Sens Ecol Conserv 10:172–187. https://doi.org/10.1002/rse2.363

Karlqvist S, Burdun I, Salko S-S, Juola J, Rautiainen M (2024) Retrieval of moisture content of common Sphagnum peat moss species from hyperspectral and multispectral data. Remote Sens Environ 315:114415. https://doi.org/10.1016/j.rse.2024.114415

Ke G, Meng Q, Finley T, Wang T, Chen W, Ma W, Ye Q, Liu T-Y (2017) LightGBM: a highly efficient gradient boosting decision tree. In: Advances in neural information processing systems. Curran Associates,

Kemppinen J, Niittynen P, Riihimäki H, Luoto M (2018) Modelling soil moisture in a high-latitude landscape using LiDAR and soil data. Earth Surf Process Landf 43:1019–1031. https://doi.org/10.1002/esp.4301

Kolari THM, Korpelainen P, Kumpula T, Tahvanainen T (2021) Accelerated vegetation succession but no hydrological change in a boreal fen during 20 years of recent climate change. Ecol Evol 11:7602–7621. https://doi.org/10.1002/ece3.7592

Kolari THM, Sallinen A, Wolff F, Kumpula T, Tolonen K, Tahvanainen T (2022) Ongoing fen-bog transition in a boreal Aapa mire inferred from repeated field sampling, aerial images, and landsat data. Ecosystems 25:1166–1188. https://doi.org/10.1007/s10021-021-00708-7

Kopecký M, Macek M, Wild J (2021) Topographic Wetness Index calculation guidelines based on measured soil moisture and plant species composition. Sci Total Environ 757:143785. https://doi.org/10.1016/j.scitotenv.2020.143785

Leifeld J, Menichetti L (2018) The underappreciated potential of peatlands in global climate change mitigation strategies. Nat Commun 9:1071. https://doi.org/10.1038/s41467-018-03406-6

Lendzioch T, Langhammer J, Vlček L, Minařík R (2021) Mapping the groundwater level and soil moisture of a montane peat bog using UAV monitoring and machine learning. Remote Sens 13:907. https://doi.org/10.3390/rs13050907

Li Z-L, Leng P, Zhou C, Chen K-S, Zhou F-C, Shang G-F (2021) Soil moisture retrieval from remote sensing measurements: current knowledge and directions for the future. Earth Sci Rev 218:103673. https://doi.org/10.1016/j.earscirev.2021.103673

Mahmood T (2024) Estimation of 100 m root zone soil moisture by downscaling 1 km soil water index with machine learning and multiple geodata. Environ Monit Assess 196:823–823. https://doi.org/10.1007/s10661-024-12969-5

Mattivi P, Franci F, Lambertini A, Bitelli G (2019) TWI computation: a comparison of different open source GISs. Open Geospatial Data Softw Stand 4:6. https://doi.org/10.1186/s40965-019-0066-y

McFeeters SK (1996) The use of the Normalized Difference Water Index (NDWI) in the delineation of open water features. Int J Remote Sens 17:1425–1432. https://doi.org/10.1080/01431169608948714

Menberu MW, Tahvanainen T, Marttila H, Irannezhad M, Ronkanen A-K, Penttinen J, Kløve B (2016) Water-table-dependent hydrological changes following peatland forestry drainage and restoration: analysis of restoration success. Water Resour Res 52:3742–3760. https://doi.org/10.1002/2015WR018578

MicaSense Knowl. Base (2023) Altum and Altum-PT Thermal Band—FAQ. https://support.micasense.com/hc/en-us/articles/360036377834-Altum-and-Altum-PT-Thermal-Band-FAQ. Accessed WWW Document

Minkkinen K, Byrne KA, Trettin CC (2008) Climate impacts of Peatland forestry. In: Strack M (ed) Peatlands and climate change. International Peat Society, Jyväskylä, pp 98–122

Mohamadzadeh N, Sadeghi M, Vergopolan N, Liang L, Bandara U, Altare C, Caldas MM (2025) Landcover-specific calibration of the optical trapezoid model (OPTRAM) for soil moisture monitoring in the Central Valley, California. Front Remote Sens 6:1519420. https://doi.org/10.3389/frsen.2025.1519420

Peng J, Loew A, Merlin O, Verhoest NEC (2017) A review of spatial downscaling of satellite remotely sensed soil moisture. Rev Geophys 55:341–366. https://doi.org/10.1002/2016RG000543

Potvin LR, Kane ES, Chimner RA, Kolka RK, Lilleskov EA (2015) Effects of water table position and plant functional group on plant community, aboveground production, and peat properties in a peatland mesocosm experiment (PEATcosm). Plant Soil 387:277–294. https://doi.org/10.1007/s11104-014-2301-8

Probst P, Wright MN, Boulesteix A-L (2019) Hyperparameters and tuning strategies for random forest. WIREs Data Min Knowl Discov 9:e1301. https://doi.org/10.1002/widm.1301

Räsänen A, Virtanen T (2019) Data and resolution requirements in mapping vegetation in spatially heterogeneous landscapes. Remote Sens Environ 230:111207. https://doi.org/10.1016/j.rse.2019.05.026

Räsänen A, Tolvanen A, Kareksela S (2022) Monitoring peatland water table depth with optical and radar satellite imagery. Int J Appl Earth Obs Geoinformation 112:102866. https://doi.org/10.1016/j.jag.2022.102866

Reddin E, Hanafin J, Tong M, Gill L, Healy MG (2025) Modelling water table depth at rewetted peatlands with Sentinel-1 and Sentinel-2. Sci Remote Sens 11:100238. https://doi.org/10.1016/j.srs.2025.100238

Rezaee M (2018) Deep convolutional neural network for complex wetland classification using optical remote sensing imagery. IEEE J Sel Top Appl Earth Obs Remote Sens 11:3030–3039. https://doi.org/10.1109/JSTARS.2018.2846178

Rodriguez-Galiano VF, Ghimire B, Rogan J, Chica-Olmo M, Rigol-Sanchez JP (2012) An assessment of the effectiveness of a random forest classifier for land-cover classification. ISPRS J Photogramm Remote Sens 67:93–104. https://doi.org/10.1016/j.isprsjprs.2011.11.002

Sadeghi M, Jones SB, Philpot WD (2015) A linear physically-based model for remote sensing of soil moisture using short wave infrared bands. Remote Sens Environ 164:66–76. https://doi.org/10.1016/j.rse.2015.04.007

Sadeghi M, Babaeian E, Tuller M, Jones SB (2017) The optical trapezoid model: a novel approach to remote sensing of soil moisture applied to sentinel-2 and landsat-8 observations. Remote Sens Environ 198:52–68. https://doi.org/10.1016/j.rse.2017.05.041

Sadeghi M, Mohamadzadeh N, Liang L, Bandara U, Caldas MM, Hatch T (2023) A new variant of the optical trapezoid model (OPTRAM) for remote sensing of soil moisture and water bodies. Sci Remote Sens 8:100105. https://doi.org/10.1016/j.srs.2023.100105

Sallinen A, Tuominen S, Kumpula T, Tahvanainen T (2019) Undrained peatland areas disturbed by surrounding drainage: a large scale GIS analysis in Finland with a special focus on aapa mires. Mires Peat 24:38. https://doi.org/10.19189/MaP.2018.AJB.391

Sims DA, Gamon JA (2002) Relationships between leaf pigment content and spectral reflectance across a wide range of species, leaf structures and developmental stages. Remote Sens Environ 81:337–354. https://doi.org/10.1016/S0034-4257(02)00010-X

Sripada RP, Heiniger RW, White JG, Crozier CR, Meijer AD (2006) Attempt to validate a remote sensing-based late-season corn nitrogen requirement prediction system. Crop Manag. https://doi.org/10.1094/CM-2006-0405-01-RS

Steenvoorden J, Limpens J (2023) Upscaling peatland mapping with drone-derived imagery: impact of spatial resolution and vegetation characteristics. GIScience Remote Sens 60:2267851. https://doi.org/10.1080/15481603.2023.2267851

Steenvoorden J, Bartholomeus H, Limpens J (2023) Less is more: optimizing vegetation mapping in peatlands using unmanned aerial vehicles (UAvs). Int J Appl Earth Obs Geoinformation 117:103220. https://doi.org/10.1016/j.jag.2023.103220

Tucker CJ (1979) Red and photographic infrared linear combinations for monitoring vegetation. Remote Sens Environ 8:127–150. https://doi.org/10.1016/0034-4257(79)90013-0

Yu Z (2011) Holocene carbon flux histories of the world's peatlands: Global carbon-cycle implications. Holocene 21:761–774. https://doi.org/10.1177/0959683610386982